Proceedings of the 5th WSEAS Int. Conf. on Signal Processing, Robotics and Automation, Madrid, Spain, February 15-17, 2006 (pp290-294)

An Approach for the Evaluation of a 3-D Ultrasound Image Reconstruction technique

Antoine Abche
Faculty of Engineering
University of Balamand
P.O. Box 100 Triploi, Lebanon

Aldo Maalouf
Electrical Eng. Dept.
University of Balamand
Tripoli Lebanon

Elie Karam
Electrical Eng. Dept.
University of Balamand
Tripoli, Lebanon

Abstract -- A method to evaluate a 3-D/2-D reconstruction technique of ultrasound images is presented. It is based on modeling and simulating the transmitted signal, the transducer, mediums through which the sound waves are propagating and the received ultrasound echoes from interfaces within the scanned object. The backscattered RF echoes are generated from a given 2-D or 3-D phantom or real images. They are collected along specified directions (defined by azimuth and elevation angles). Then, they are fed as input to an image reconstruction approach based on a beamforming technique and a frequency-time distribution approach, namely, the Wigner Ville Distribution (WVD). The original and the reconstructed images are compared to evaluate the reconstruction approach.

Keywords – Reconstruction, Evaluation, Simulation, Wigner Ville, Ultrasound, modeling

1 Introduction

Diagnostic ultrasound has been used for more than fifty years. Nowadays, it has become one of the most popular medical diagnostic tools. It has the advantage of safety, low cost and interactivity, compared to other imaging modalities such as X-ray Computed Tomography (CT) and Magnetic Resonance Imaging (MRI). The acquisition of 3-D images that resemble the idealized pictures of anatomy books has leaded the researchers to develop 3-D ultrasound imaging. It offers a number of advantages over 2-D imaging: i) it allows the visualization of the 3-D nature of the imaged organ or structure, ii) it expands the Field Of View (FOV) to allow the presentation of neighbouring anatomy, iii) it allows the visualization of 2-D cross sectional images at angles impossible to achieve by prior examination, iv) it allows an accurate quantitative measurement of the organ's size or volume and v) it implies the potential to reduce some of the artifacts present in a 2-D scan such as shadow, speckle and reverberation.

Various approaches have been developed to acquire and visualize 3-D information collected by the ultrasound imaging modality including real time volumetric ultrasound imaging. One approach is based on the implementation of 2-D array of sensors [1-3], a "handheld motorized" set up to acquire a set of parallel slices [4] or a free hand system to collect non-parallel slices [5] to reconstruct a 3-D volume. Alternative approaches involve reflective and transmission modes of Ultrasound Computed Tomography (UCT) [6]. That is, images of ultrasonic reflectivity and ultrasonic attenuation are reconstructed using reconstruction algorithms developed for X-ray CT. In the latter mode, the time of flight's (TOF) measurements are useful in the reconstruction of images of the refractive index within the imaged region and consequently the speed of sound distribution.

In this work, an approach to evaluate a 2-D or 3-D reconstruction technique of ultrasound images is presented. This approach involves the generation of RF echoes from the acquired ultrasound images, the modeling of the transducer, the modeling of the medium, the attenuation and reflection of the ultrasound beam. Consequently, the generated echoes are fed as input to evaluate a particular reconstruction technique. The reconstruction of the ultrasound images is achieved using the Wigner Ville distribution to analyze the echoes and localize the interfaces along the path of the beam.

2 Method

The approach assumes a phased two-dimensional array of ultrasound sensors with a Field Of View

(FOV) that has a pyramidal shape (Figure 1). The center $(x_c, y_c, 0)$ of the array of sensors is assumed to coincide with the center of the pyramidal scan in the xy plane. Any point inside the pyramidal FOV is described by the azimuth angle ψ (the steering angle in the azimuth direction), an elevation angle θ (steering angle in the elevation angle) and the distance in the radial direction (ρ). They are related to the corresponding Cartesian coordinates (x,y,z) by:

$$\rho = \sqrt{(x - x_c)^2 + (y - y_c)^2 + z^2} \tag{1}$$

$$x = z \tan \psi \tag{2}$$

$$y = z \tan \theta \tag{3}$$

Azimuth and Elevation angles are measured with respect to the normal at the center of the 2-D array. The array spacing and the dimensions of sensors impose restrictions on the maximum angles in the azimuth and elevation directions. Exceeding the maximum steering angles will cause spatial aliasing and, consequently, image artifacts.

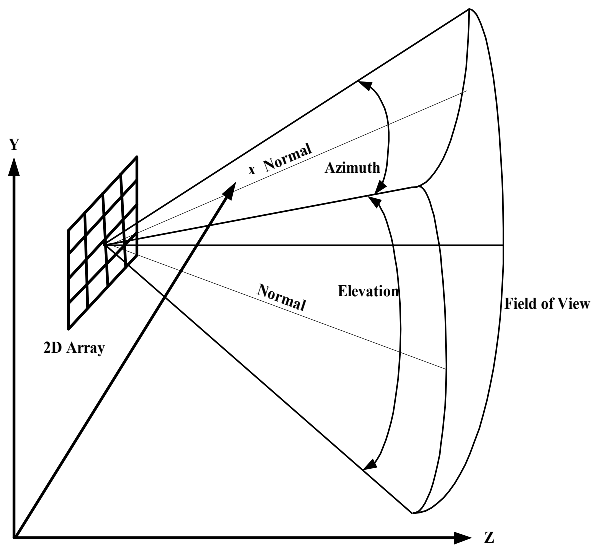

Figure 1: Pyramidal field of view

2.2 Acoustic wave modeling

The model of the acoustic wave in tissue or a medium through which a wave is propagating is described by the Helmholtz equation for the spatially dependent variable P [9]:

$$\nabla_p^2 = \frac{1}{c^2}\frac{\partial^2 P}{\partial t^2} \tag{4}$$

Where c is the velocity of sound in the medium in m/s, P is the pressure in Pa and t is the time in second. This function is the result of a linearization using the Born approximation of the first order.

2.3 Model of the transducer

Various models of piezoelectric transducers have been developed and can be found in the literature [10-12]. These models allow the selection of the optimized parameters characterizing the transducer as well as the evaluation of their effects. In this work, the KLM model operating in the thickness mode has been implemented (Figure 2). It consists of an equivalent circuit made of three ports: one electric port and two acoustic ports separated by an ideal electromechanical transformer. The latter two ports represent the front and back faces of the transducer. The transducer's transfer function is described by $1/Z_{KLM}$ where Z_{KLM} is the equivalent electric impedance of the transducer [12].

2.4 Transmitted signal

The transmitted signal is assumed to be a sinusoidal signal having a frequency ($w_0 = 2\pi f_0$) and is equal to the transducer's operating frequency (or the transducer's center frequency). The length of the transmitted pulse, known as the Spatial Pulse Length (SPL), is dependent on the axial resolution. Each ultrasound signal is transmitted along a particular direction defined by steering angles (ψ and θ). Thus, the number of rays to cover the Field of View (FOV) of the acquired image (and consequently the resolution) must be defined.

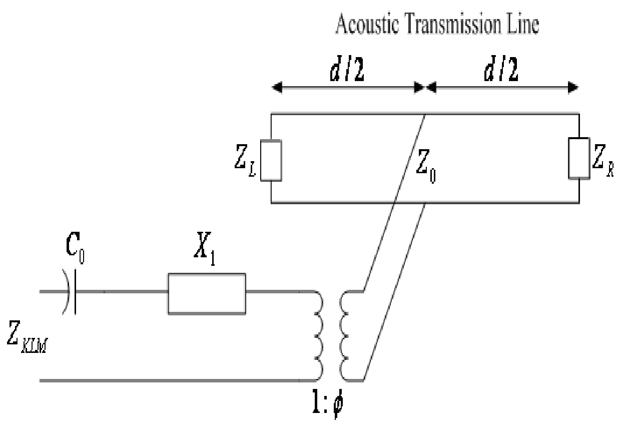

Figure 2: KLM Model of the transducer

2.5 Reflection and attenuation

When a transducer transmits an ultrasonic wave along a path through the patient, multiple interfaces are encountered along the path of the ultrasound beam. A percentage of the beam intensity will be reflected at the interface and collected by the transducer, and another percentage will be transmitted until it encounters another interface. These percentages depend on the acoustic impedance mismatch (Z_1 and Z_2) between the two mediums separating a particular interface.

On the other hand, the attenuation of the beam intensity through the various mediums along its path is taken into account. It includes the effects of both scattering and absorption of the beam.

2.6 Model of the Medium

Since the ultrasonic wave is propagating through different mediums, the various mediums along each ray must be simulated. In this regard, an impedance value must be associated with each voxel. The acoustic impedance is the same in successive pixel/volume elements within a homogeneous medium. Otherwise, a new value of the acoustic impedance is assigned. The result is a vector of acoustic impedances. Each impedance value is disturbed by a small value randomly and independently to simulate the tissue inhomogeneities.

2.7 Generation of backscattered echoes

The received RF signal s(t) is computed by convolving the transducer excitation function with the spatial impulse response (transfer function) of the electro-mechanical transducer during the transmission and reception of the pulse. The result is convolved with the acoustic impedance vector along the corresponding ray. The received RF signal is given by [13]:

$$s(t) = \int_{-\infty}^{\infty} \frac{Z_A}{Z_{KLM}} \left[\frac{\pi}{j} \left(\delta(w - w_0) + \delta(w + w_0) \right) \right] e^{jwt} dw \qquad (5)$$

3 Reconstruction

The simulated ultrasound echoes are fed as input to a reconstruction algorithm of ultrasound images to evaluate its performance. The approach is based on the localization of the interfaces using the Wigner Ville Distribution (WVD) and a phase shift beam former technique [8].

The collected echoes are fed into a variable gain amplifier to perform the time gain compensation process. The corresponding output is demodulated by multiplying the signal by e^{-jw0t} (w_0 is the demodulation frequency) to produce the real and imaginary components (quadrature and in phase components). Each output is filtered by a low pass filter. Then, the results are fed into a unit in which the signal is phase shifted. The amount of phase shift is determined by the steering angles and the position of the received crystal in the array. Then, the signal is reconstructed by multiplying the real output with a $\cos(w_o t)$ and the imaginary output by a $\sin(w_0 t)$. The results of both operations are combined and filtered using a FIR low pass filter. At this stage, the localization of the interfaces is performed (Figure 3). The analysis is based on a joint time-frequency technique, namely, the Wigner Ville Distribution (WVD). It is defined by [14]:

$$W_x(nT,f) = 2T \sum_{l=-L}^{L} x(nT+lT)x^*(nT-lT)w(l)w^*(-l)e^{-j4\pi fl} \qquad (6)$$

Where w(l) is a window sequence.

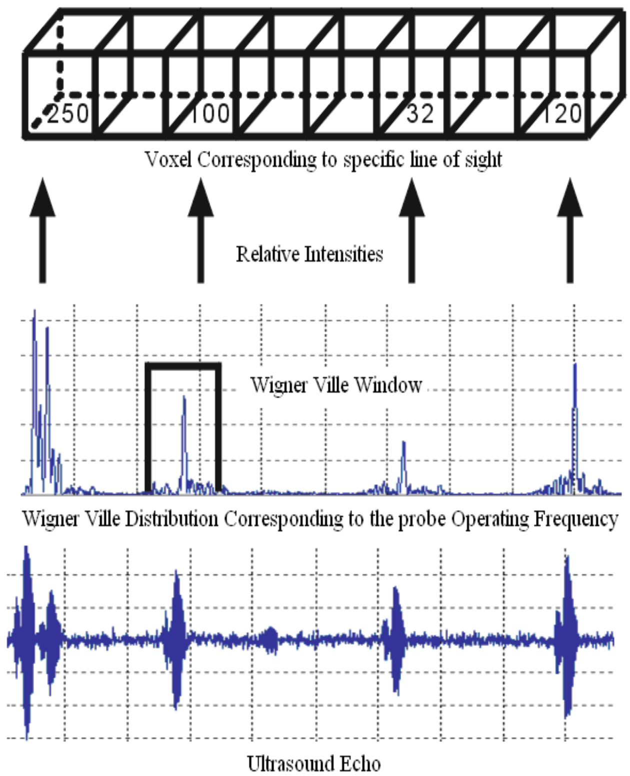

Figure 3: Processing of the returned echo using WVD.

Having localized the interfaces along a ray and defined the resolution of each voxel along the x, y and z directions, the corresponding voxels in a Cartesian coordinate system are identified and

Proceedings of the 5th WSEAS Int. Conf. on Signal Processing, Robotics and Automation, Madrid, Spain, February 15-17, 2006 (pp290-294)

assigned the appropriate intensity values. The intensity value is proportional to the peak value of the signal in the window of the WVD (Figure 3). The procedure is repeated for each line of sight to form the 3-D image.

4 Results

The approach is evaluated using a real 2-D image of the heart of a patient. The raw data are collected using the ALOKA 2200S ultrasound scanner. The probe of the ALOKA 2200S is a phased linear array that consists of 64 transducers. Each transducer is operating at a frequency of 3.32 MHz. The data is acquired by firing one crystal at a time and receiving the echoes detected by all 64 transducers. A total of 4096 "A scans" is acquired covering the whole FOV. The data are collected by the Biomedical Ultrasonic Laboratory at the University of Michigan. Figure 4 shows the original 2-D image of the heart.

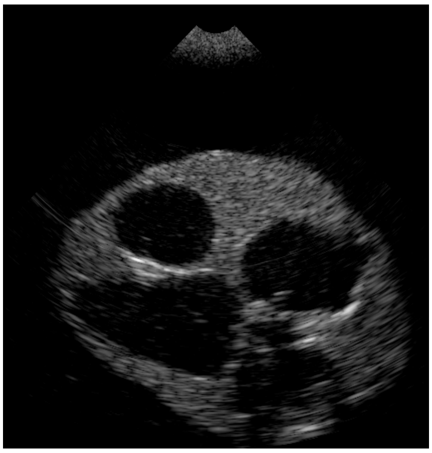

Figure 4: Original 2-D image of the heart of a patient

Figure 5 shows a typical original RF ultrasound echo received by the real array of sensors (i.e. the ALOKA 2200S ultrasound scanner). The corresponding simulated RF echo is illustrated in Figure 6. They are acquired along the direction defined by the steering angles $\theta = \psi = 0°$. The two signals are comparable. Similar results have been observed by comparing corresponding echoes along other steering angles.

Having generated the simulated RF backscattered echoes, a phased shift beamforming technique is performed on the acquired data set before the localization of the interfaces along each ray is achieved using the WVD. Each pixel is assigned an intensity value that is proportional to the peak value within the window of the WVD. Figure 7 shows the result of the implementation of the approach outlined earlier. It is clear that the reconstructed image is similar to the original image. The error is computed as the ratio of the number of non-zero voxels in the difference image and the total number of voxels. The error was found to be equal to 0.24414 %.

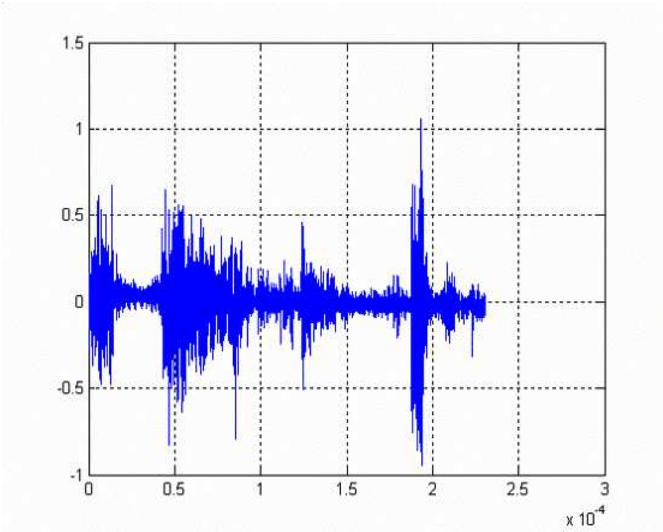

Figure 5: Original RF echo acquired by the actual transducers along $\theta = \psi = 0°$.

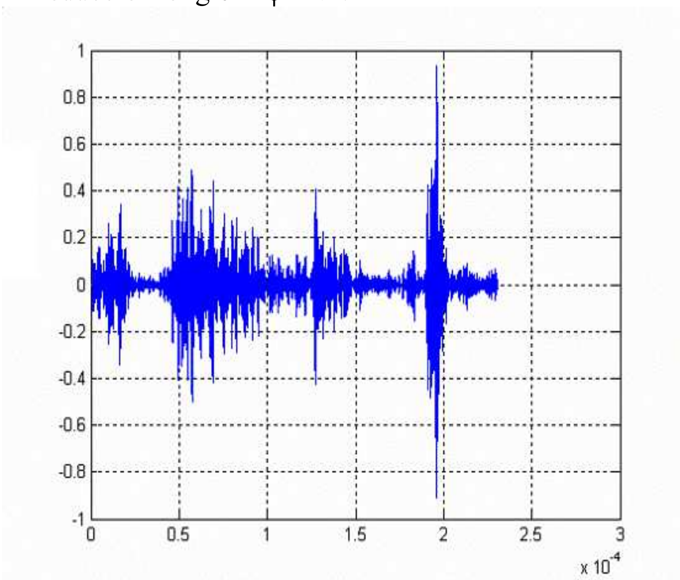

Figure 6: Simulated RF echo along $\theta = \psi = 0°$.

Figure 7: Reconstructed image of the heart.

5 Conclusion

In this paper, a method to evaluate a 3D ultrasound image reconstruction technique is implemented. The approach generates the simulated backscattered echoes along different steering angles by taking into account the model of the transducer, the model of the propagating wave, the reflection as well as the attenuation of the ultrasonic wave as it propagates through the medium. This approach can be easily accommodated for a 2-D image by selecting the elevation angle to be equal to zero. The results reveal the proposed approach is successful.

References:

[1] S. W. Smith, H. G. Pavy, and O. T. von Ramm. High speed ultrasound volumetric imaging system-part I: Transducer design and beam steering, *IEEE Trans. Ultrason., Ferroelect., Freq. Contr.*, 38:100–108, 1991.

[2] S. W. Smith, H. G. Pavy, and O. T. von Ramm. High speed ultrasound volumetric imaging system-part II: Parallel processing and image display. *IEEE Trans. Ultrason., Ferroelect., Freq. Contr.*, 38:109–115, 1991.

[3] O. Oralkan, C. H. Cheng, J. Johnson, M. Karaman, T. H. Lee, and B. T. Khuri Yakub. Volumetric ultrasound imaging using 2-D CMUT arrays. *IEEE Trans. Ultrason., Ferroelect., Freq. Contr.*, 50:109–115, 2003.

[4] C. Neale, J. D. Gill, and F. Aaron. Analysis of geometrical distortion and statistical variance in length, area, and volume in a linearly scanned 3D ultrasound image. *IEEE Transactions on Medical Imaging*, 19, 2000.

[5] J. Sanches, J. Marques, F. Pinto, and P. Ferreira. A 3d ultrasound system for medical diagnosis. *IEEE Transactions on Medical Imaging*, 19, 2002.

[6] F. Anderson. 3D real time ultrasonic imaging using ellipsoidal backprojection. *Proceedings of SPIE*, 1443:62–80.

[7] Wang X., Ritchie C. J. & Kim Y. (1996, June). Elevation direction deconvolution in three dimensional ultrasound imaging. *IEEE Trans. Med. Imag.*, *vol. 15, pp. 389–394*

[8] K. E. Thomenius, "Evolution of ultrasound beamformers," in *Proc. IEEE Ultrason. Symp.*, 1996, pp. 1615–1622.

[9] Tomi H., Matti M., Jari P. K., Phillip J. White & Kullervo H. A Full-Wave Helmholtz Model for Continuous-Wave Ultrasound Transmission

[10] Willatzen M., Ultrasound Transducer modeling, General Theory and Applications to Ultrasound Reciprocal Systems, IEEE Transactions on Ultrasonics, Ferroelectrics, and Frequency Control, Vol 48, January 2001.

[11] Desilets C. S., Fraser J. D. and Kino G. S., The Design of Efficient Broad-Band Piezoelectric Transducers, IEEE Trans. Son. Ultrason., Vol SU-25,pp. 115-125, 1978.

[12] S. Stewart, P. L. Sean, P.D. Benjamin and Y. Cohen, Comparison of the Mason and KLM Equivalent Circuits for Piezoelectric Resonators in the Thickness Mode, *IEEE Ultrasonic Symposium*, 1999.

[13] Meunier J. & Bertrand M. (1995). Echographic Image Mean Gray Level Changes With Tissue Dynamics: A System Based Model Study. *IEEE Transactions on Biomedical Engineering, (42)*

[14] Qian Shie and Chen Dapang. *Joint Time Frequency Analysis Methods and Applications*. Prentice Hall Inc., Upper Saddle River, NJ 07458, USA, 1996.